RESEARCH ARTICLE | JANUARY 08 2014

Coexistence of synchrony and incoherence in oscillatory media under nonlinear global coupling

Lennart Schmidt; Konrad Schönleber; Katharina Krischer; Vladimir García-Morales

Chaos 24, 013102 (2014)
https://doi.org/10.1063/1.4858996

Coexistence of synchrony and incoherence in oscillatory media under nonlinear global coupling

Lennart Schmidt,[1,2] Konrad Schönleber,[1] Katharina Krischer,[1,a)]
and Vladimir García-Morales[1,2]
[1]*Physik-Department, Nonequilibrium Chemical Physics, Technische Universität München, James-Franck-Str. 1, D-85748 Garching, Germany*
[2]*Institute for Advanced Study, Technische Universität München, Lichtenbergstr. 2a, D-85748 Garching, Germany*

(Received 18 October 2013; accepted 16 December 2013; published online 8 January 2014)

We report a novel mechanism for the formation of chimera states, a peculiar spatiotemporal pattern with coexisting synchronized and incoherent domains found in ensembles of identical oscillators. Considering Stuart-Landau oscillators, we demonstrate that a nonlinear global coupling can induce this symmetry breaking. We find chimera states also in a spatially extended system, a modified complex Ginzburg-Landau equation. This theoretical prediction is validated with an oscillatory electrochemical system, the electro-oxidation of silicon, where the spontaneous formation of chimeras is observed without any external feedback control. © *2014 AIP Publishing LLC*. [http://dx.doi.org/10.1063/1.4858996]

In the 17th century, Christiaan Huygens was the first who encountered the phenomenon of synchronization, when watching two coupled pendulum clocks adjusting their oscillation phase to each other. Since then, a variety of systems exhibiting synchronization were studied, e.g., the flashing of fireflies or networks of pacemaker cells keeping our heart beating in time. In these systems, the key aspect is that nonidentical oscillating elements, as nature is never perfect, with a distribution of natural frequencies become synchronized due to the mutual coupling. In contrast, in 2002, Kuramoto and Battogtokh[1] found the opposite phenomenon: a perfect symmetric system of identical oscillators coupled via a nonlocal coupling (i.e., a coupling that somehow decreases with the distance between two oscillators) may undergo a transition to a state, where a synchronized group of oscillators coexists with an unsynchronized one. This situation was later named chimera state, since the chimera was, according to Greek mythology, composed of the parts of different animals. The nonlocality of the coupling is believed to be indispensable for the formation of chimera states. However, in the present article, we show that this is a misbelief, as we found chimera states under solely global coupling. Global coupling means that each individual oscillator couples to the mean field of all oscillators. In our case, the mean field is a nonlinear function of the state variables of each oscillator.

I. INTRODUCTION

An oscillatory medium experiencing a global coupling or feedback mechanism may evolve towards a domain-like structure, called a cluster state, in which each domain oscillates uniformly with a defined phase difference to the others.[2] Several theoretical studies on nonlocally coupled oscillatory systems predicted a strange domain-type pattern, a so-called chimera state, where some domains are perfectly synchronized, but others oscillate spatially incoherently.[1,3–11] Chimera states might be of importance for some peculiar observations in different disciplines, such as the unihemispheric sleep of animals,[12,13] the need for synchronized bumps in otherwise chaotic neuronal networks for signal propagation,[14] and the existence of turbulent-laminar patterns in a Couette flow.[15] Very recently, the existence of chimera states could be validated in two pioneering experiments with chemical[16] and optical oscillators.[17] Both experiments involved a specifically designed feedback algorithm to generate the specific nonlocal coupling. Subsequently, chimera states could be realized in systems of mechanical[18] and electrochemical[23] oscillators. However, experimental evidence of the spontaneous formation of chimera states without the control from outside is still missing.

In this article, we demonstrate, both theoretically and experimentally, that also under a strictly global coupling, if being nonlinear, a coexistence of synchrony and asynchrony can be found. We start with an ensemble of Stuart-Landau oscillators interacting solely via a nonlinear global coupling. An initially random distribution splits for given parameters into two groups, one being synchronized and the other one being desynchronized. We then discuss spatially extended oscillatory media. We show that a modified complex Ginzburg-Landau equation (MCGLE) with nonlinear global coupling, originally proposed to explain special cluster patterns observed during the oscillatory electro-oxidation of silicon in fluoride containing electrolytes,[19,20] describes a transition from cluster patterns to a state with coexisting synchronized and incoherent domains. The results are indeed confirmed experimentally with the oscillating Si-system, where the separation of the electrode into coherently and incoherently oscillating domains occurs spontaneously and without external feedback control. Most remarkably, the incoherent region does not contain any amplitude defects.

a)krischer@tum.de

All these are essential properties of chimera states and we conclude that we have found a novel mechanism to this symmetry-breaking state. Moreover, since a global coupling is frequently encountered, chimera states might exist in many more systems than anticipated so far.

II. RESULTS AND DISCUSSION

A. Chimera states in an ensemble of Stuart-Landau oscillators

First, we consider an ensemble of N Stuart-Landau oscillators[21] under nonlinear global coupling

$$\frac{\mathrm{d}}{\mathrm{d}t}W_j = W_j - (1+ic_2)|W_j|^2 W_j - (1+i\nu)\langle W\rangle + (1+ic_2)\langle |W|^2 W\rangle\,, \qquad (1)$$

where $j \in [1,N]$ labels each individual oscillator and $\langle W\rangle = \sum_{k=1}^{N} W_k/N$ and $\langle |W|^2 W\rangle = \sum_{k=1}^{N} |W_k|^2 W_k/N$ denote ensemble averages. The first term on the right hand side is the linear instability leading to oscillations, while their magnitudes are controlled by the cubic term. The last two terms represent the nonlinear global coupling. Taking the ensemble average on both sides of Eq. (1) yields $\mathrm{d}\langle W\rangle/\mathrm{d}t = -i\nu\langle W\rangle$ and thus $\langle W\rangle = \eta\exp(-i\nu t)$, i.e., the average $\langle W\rangle$ exhibits conserved harmonic oscillations with amplitude η and frequency ν. As we will see later, this conservation law strongly influences the dynamics. Altogether we have three parameters, namely c_2, ν and η.

We numerically solved Eqs. (1) (for details, see the Appendix). Starting from a random distribution, for $c_2 = -0.6$, $\nu = 0.02$, $\eta = 0.7$, and $N = 1000$, the ensemble splits into two groups as depicted in Fig. 1, where we show the real parts of W_j for all oscillators. One group is synchronized (red, light gray) and the other group is desynchronized (blue, dark gray). The synchronized oscillators perform collective and nearly harmonic oscillations, while the asynchronous ones exhibit incoherent and irregular motions. Although the oscillations of this latter group present a seemingly regular spiking, the oscillators in this group are strongly uncorrelated both in time and in their simultaneous amplitudes and phases. We observe strong amplitude fluctuations in the incoherent group, as this is also the case for chimeras found in a nonlocally coupled system in a parameter region, where the weak-coupling approximation does not apply.[22]

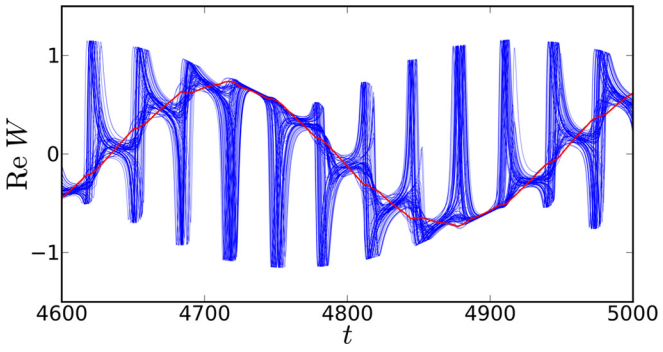

FIG. 1. Time series for the real parts of W_j for all oscillators are shown. The synchronized oscillators (red, light gray) perform collective and nearly harmonic oscillations, while the asynchronous oscillators (blue, dark gray) exhibit incoherent and irregular dynamics. For parameters see text.

The regularity of the spiking can be explained by a second time-scale inherent in the system. As discussed for the continuous system in Ref. 20, in the parameter regime, where clustering occurs, the nonlinear global coupling leads to two dominant time-scales: the frequency ν of the oscillation of the spatial average and a frequency, which may be called the cluster frequency. The contribution to the oscillations in the two phases at this cluster frequency shows a phase shift of π (between the two phases). The time-scale of the spiking in Fig. 1 is given by the cluster frequency described above as the clustering mechanism leads to the separation into the two groups. Interestingly, chimera states found in an electrochemical experiment with individual electrodes arranged on a ring and coupled nonlocally exhibit a similar spiking behaviour: the desynchronized oscillating elements drift some time with the mean-field, interrupted by fast 2π phase slips.[23]

In essence, we have found the coexistence of synchrony and asynchrony, i.e., a kind of a chimera state, evolving under a solely global coupling. This contradicts the assumption that a nonlocal coupling is indispensable for the occurrence of these states. Contrarily to the findings in Ref. 24, the chimera state is stable independently of the population size and forms spontaneously[25] from a random distribution. The co-existing synchronized state is unstable, which is also the case for the chimera states described in Refs. 22 and 25. In the latter work, it is argued that this is connected with strong fluctuations of the amplitude in the incoherent region, as they did not consider the weak-coupling limit. The type of chimera states found here are absent under linear global coupling.[26] Note, however, that linear global coupling may induce other types of chimera states, also in an ensemble of Stuart-Landau oscillators involving large amplitude variations,[27] or in a globally coupled map lattice.[28] The former state can also be found in our model, Eq. (1), and will be discussed elsewhere.

B. Transition to a chimera state in the modified CGLE

In order to describe experiments on a spatially extended oscillatory medium, we consider now the MCGLE,[19,20]

$$\partial_t W = W + (1+ic_1)\nabla^2 W - (1+ic_2)|W|^2 W - (1+i\nu)\langle W\rangle + (1+ic_2)\langle |W|^2 W\rangle\,. \qquad (2)$$

Here, $W(\mathbf{r},t)$ is the complex order parameter describing the dynamical state at each point $\mathbf{r} = (x,y)$ at time t and $\langle\ldots\rangle$ now denotes the spatial average. The original complex Ginzburg-Landau equation without the nonlinear global coupling is a generic model for extended systems at the onset of oscillations and has a wide range of applications.[29] The MCGLE, Eq. (2), was proposed to explain experimental results of the electro-oxidation of n-Si(111) under illumination.[19] In fact, the emergence of subharmonic cluster patterns

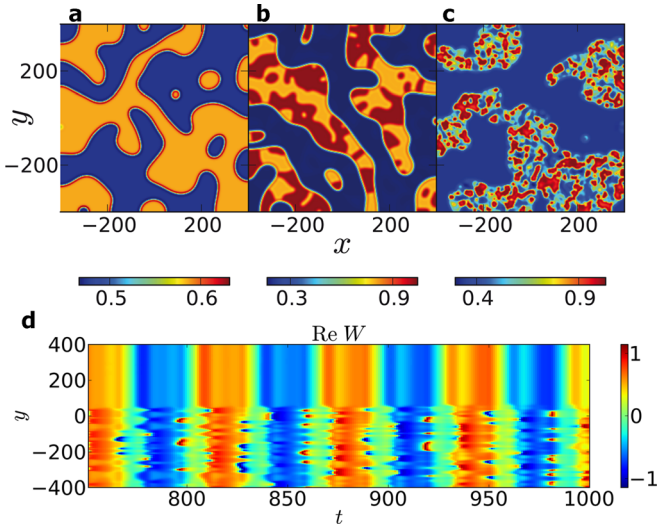

FIG. 2. (a)–(c) Snapshots of the three cluster-states. Shown is the real part of the complex order parameter Re W, calculated from Eq. (2), indicating the dynamical states of each local oscillator. (a) Two-phase clusters obtained for parameter $c_2 = -0.7$. Both phases are homogeneous. (b) Sub-clustering at $c_2 = -0.67$. In this case, one phase is homogeneous, while the other one splits again into two-phase clusters. (c) Two-dimensional chimera state found for $c_2 = -0.58$. The inhomogeneous phase shows strongly incoherent dynamics. (d) Temporal evolution of the real part of W in a cut along the y-direction at $x = 0$ in (c). Perfectly synchronized motion coexists with asynchronous behaviour, separated by a sharp boundary.

in the oxide-layer thickness at the silicon-electrolyte interface can successfully be described by Eq. (2).[20] An important experimentally observed feature is a nearly harmonic oscillation of the spatially averaged oxide-layer thickness. This is captured by the conservation law for the homogeneous mode $\langle W\rangle = \eta\exp(-i\nu t)$ in the theory.[20]

We numerically solved Eq. (2) (for details, see the Appendix) for fixed parameters $c_1 = 0.2$, $\nu = 0.1$, and $\eta = 0.66$. For appropriate values of c_2, the system splits into two phases, as presented in Fig. 2(a) for $c_2 = -0.7$.

The specific interaction between these two phases via the nonlinear global coupling leads to a symmetry-breaking transition, as we will show in the following. Let us call the two phases A and B, respectively. Simulations show that the system evolves according to a minimization of the interface between A and B. This leads to a demixing of the phases. As the diffusional coupling between A and B acts only near the boundaries, for large domain sizes, it can be neglected. Under this assumption, the dynamics in each phase is governed by

$$\partial_t W_X(\mathbf{r},t) = W_X(\mathbf{r},t) + (1+ic_1)\nabla^2 W_X(\mathbf{r},t) - (1+ic_2)|W_X(\mathbf{r},t)|^2 W_X(\mathbf{r},t) + Z(W_A,W_B)\,, \tag{3}$$

where X = A, B and $Z(W_A, W_B)$ is the coupling between A and B and has to be determined. Exploiting the conservation law for the homogeneous mode, one finds

$$Z(W_A,W_B) = -(1+i\nu)\eta\exp(-i\nu t) + (1+ic_2)\frac{1}{2}\left(\langle|W_A|^2W_A\rangle + \langle|W_B|^2W_B\rangle\right). \tag{4}$$

We can further write for the spatial averages over phases A and B $R_A\exp(-i\alpha) \equiv \langle|W_A|^2W_A\rangle$ and $R_B\exp(-i\beta) \equiv \langle|W_B|^2W_B\rangle$, respectively, and $K\exp(i\gamma) \equiv (1+ic_2)/2$, where $\gamma = \gamma(c_2)$. With the phase difference $\Delta\phi \equiv \beta - \alpha$ between A and B, one can now show that the intra-group coupling differs from the inter-group coupling. Note that $\Delta\phi$ is generally unequal to π as we are dealing with subharmonic two-phase clusters.[19,20] One obtains in terms of α

$$Z(W_A,W_B) = -(1+i\nu)\eta e^{-i\nu t} + KR_A e^{i(\gamma-\alpha)} + KR_B e^{i(\gamma-\Delta\phi-\alpha)}\,. \tag{5}$$

We see that phases A and B experience each a different influence from the intra- and inter-group couplings. This is not due to a difference in coupling strength defined a priori, but is the result of the intrinsic dynamics causing the phase difference. As studies of two subpopulations in Refs. 7 and 16 with global intra- and inter-group couplings of different strength show the existence of chimera states, we conclude that the similar situation arising here renders the emergence of chimeras possible. The coupling can be tuned with the parameter c_2, where the influence is different on inter- and intra-group coupling if $\Delta\phi$ depends also on c_2, which is a reasonable assumption.

As presented in Fig. 2, we find three remarkable, stable states. As already mentioned, for $c_2 = -0.7$, Fig. 2(a), we observe two-phase clusters. By changing to $c_2 = -0.67$, shown in Fig. 2(b), one finds A being homogeneous and B exhibiting two-phase clusters as a substructure. Finally, we observe a chimera state for $c_2 = -0.58$, where B becomes turbulent. This is depicted in Fig. 2(c). All these states were also found in Ref. 16, but there the two subpopulations were man-made and the system had to be initialized in a special manner. In contrast, in our case, the system splits spontaneously into the two groups.

To further illustrate the characteristics of the chimera state, we show the spatio-temporal dynamics in a cut along the y-direction versus time in Fig. 2(d). It demonstrates the separation into two parts, one being perfectly synchronized, while the other one exhibits asynchronous behaviour. The individual oscillators in the homogeneous region oscillate periodically, while in the inhomogeneous region, the dynamics is irregular, but still slaved to the oscillation of the mean value $\langle W\rangle$ due to the conservation law. As in the ensemble of Stuart-Landau oscillators, the chimera state is stable in the MCGLE.

Now, we turn towards the experimental situation, which had led to the formulation of the modified CGLE, Eq. (2).

C. Experimental validation of theoretical prediction

The system investigated is the photoelectrochemical dissolution of n-type doped silicon in fluoride containing electrolytes. Here, the silicon sample is oxidized electrochemically via the following dominant reaction:[30]

$$\begin{aligned}&\mathrm{Si} + 4\mathrm{H_2O} + \nu_{\mathrm{VB}}\mathrm{h}^+ \rightarrow \mathrm{Si(OH)_4} + 4\mathrm{H}^+ + (4-\nu_{\mathrm{VB}})\mathrm{e}^-\\ &\mathrm{Si(OH)_4} \rightarrow \mathrm{SiO_2} + 2\mathrm{H_2O},\end{aligned} \tag{6}$$

where (ν_{VB}) represents the number of charge-carriers transferred through valence-band processes and $(4-\nu_{\mathrm{VB}})$ the

number of charge-carriers transferred through conduction-band processes. The second reaction is solely chemical, i.e., no charge-carriers are transferred for the reaction. It has to be noted that the initial charge transfer is always a valence-band process rendering illumination necessary for the reaction to occur at n-type doped silicon samples. The illumination also limits the total current, which is a likely source of the non-linear global coupling.[31]

The generated oxide is etched away by the fluoride species present in the electrolyte, e.g., HF,[32] in another solely chemical process

$$SiO_2 + 6HF \rightarrow SiF_6^{2-} + 2H^+ + 2H_2O. \quad (7)$$

As silicon oxidation and the etching of silicon oxide have opposite effects on the oxide-layer thickness, a steady state can be reached for suitable experimental conditions. Already in the 1950s, it was found that the system can also be oscillatory, which has drawn a lot of attention since then (for a review, see chapter 5 in Ref. 33). The current oscillations are accompanied by an oscillating oxide-layer thickness with an amplitude in the nm-range.[34–38]

To investigate the spatial distribution of the oxide-layer thickness during the oscillations, we use spatially resolved ellipsometric imaging, a technique first established by Rotermund *et al.*,[39] with a setup described in the Appendix. The elliptical polarization of a light beam is distorted upon reflection from the working electrode surface by the silicon oxide layer and these distortions are translated into a two-dimensional representation of the oxide-layer thickness on the surface.

It was found that spatial pattern formation with a rich variety of different patterns occurs on n-type doped silicon samples at intermediate illumination intensities.[19,40] An external resistor in series with the working electrode acts as an additional linear global coupling.[41]

In Figs. 3(a)–3(c), we present experimentally measured snapshots of the oxide-layer thickness. Consistent with the theory, Fig. 2(a), the case of two-phase clusters is shown in Fig. 3(a).

As visible in Fig. 3(b), we also observe a sub-clustering in the experiment as in Fig. 2(b). A stripe exhibiting two-phase clusters is embedded in an otherwise homogeneous region, which oscillates twice as fast as the two-phase clusters.

Finally and most remarkably, also the spontaneous formation of a two-dimensional chimera state occurs in the experiments, Figs. 3(c) and 3(d). As apparent in the snapshot (Fig. 3(c)) and the time evolution of a one-dimensional cut (Fig. 3(d)), the upper right corner of the electrode constitutes the synchronized region, whereas the remaining part displays turbulent dynamics. A one-dimensional snapshot of the oxide-layer thickness in Fig. 4(b), with corresponding distribution visualized by a histogram, shows the strong variations in the incoherent region.

We found the coexistence of synchrony and incoherence for several experimental parameters. For sufficiently long measurement times, we observed a transient nature. On the contrary, for all considered simulation durations, the chimera state remains stable in the ensemble of Stuart-Landau oscillators, Eq. (1), and in the MCGLE, Eq. (2), for the given parameter values.

We have to point out that, as in the simulations, nothing is imposed onto the system to introduce the splitting into two domains. This separation arises solely from the intrinsic dynamics. We remark as well that there is no Turing-Hopf bifurcation[42] or an analogous situation that would trigger the splitting. Furthermore, great care was taken to assure that the

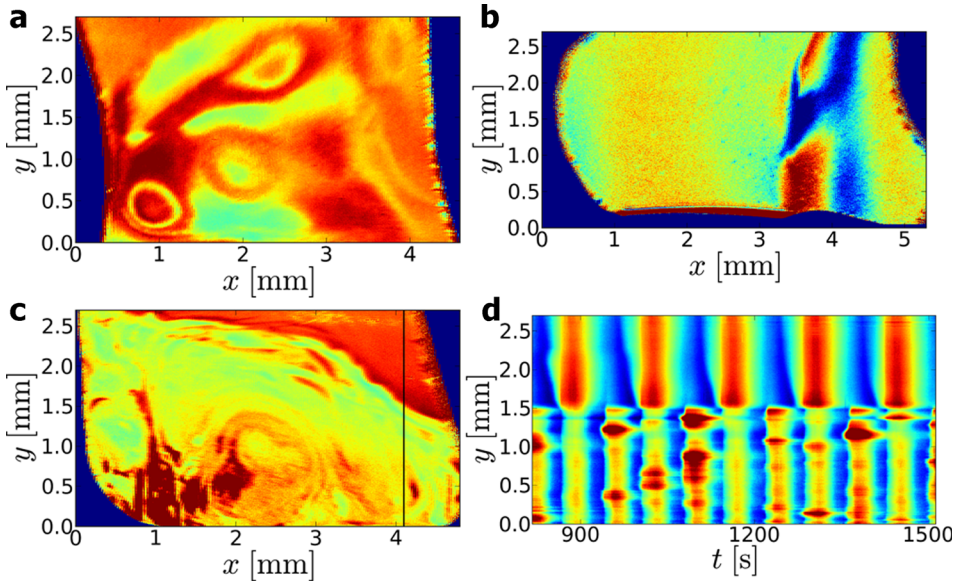

FIG. 3. Spatio-temporal evolution of the oxide-layer thickness during the electrodissolution of silicon: two-phase clusters, sub-clustering and chimera state. Shown are snapshots, colours indicate the thickness of the oxide layer, x and y represent spatial coordinates and t denotes time. (a) Two-phase cluster state, where both parts oscillate uniformly with a phase difference to the respective other. (b) The oxide-layer thickness exhibits sub-clustering: a stripe of two-phase clusters is embedded in an otherwise uniformly oscillating background. The clusters in the stripe oscillate at half the frequency of the background oscillation. (c) Chimera state: the coexistence of synchrony and asynchrony is apparent. (d) Cut along y (black line in (**c**)) showing the sharp separation into coherent and incoherent regions. For experimental parameters, see the Appendix.

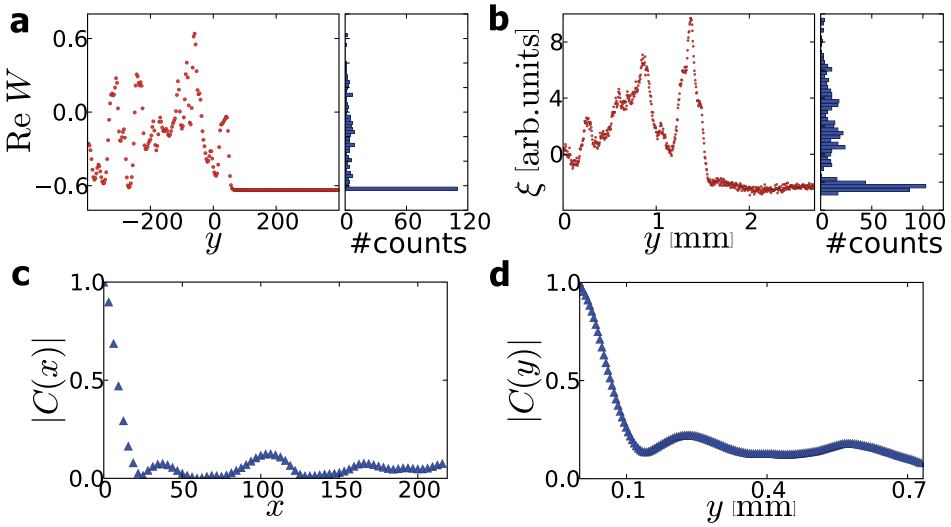

FIG. 4. Comparison of theoretical and experimental chimera states. The one-dimensional spatial profiles and histograms in theory (a) and experiment (b) are in excellent agreement. Furthermore, both correlation functions $|C(x)|$ (for details, see text) exhibit a fast drop to nearly zero. This shows the fast decrease of spatial correlations in theory (c) and experiment (d).

experimental conditions are spatially uniform. To this end, the electrolyte is stirred continuously and the counter electrode is placed symmetrically in front of the silicon working electrode.

Finally, we make a direct comparison of the theoretical and experimental spatial profiles of the real part of W in Fig. 4(a) and the oxide-layer thickness ξ in Fig. 4(b), respectively. These plots show an excellent qualitative agreement.

Furthermore, we quantified the incoherence in the turbulent regions of the chimera state: we calculated the correlation function $C(x,t) = \langle \tilde{W}(x,t)\tilde{W}^*(0,0)\rangle_{x',t'} / \langle |\tilde{W}(0,0)|^2 \rangle_{x',t'}$ (the asterisk denotes complex conjugation and the average is performed over space and time) in a cut in the incoherent region for both theory and experiment, where $\tilde{W}$ is obtained by subtracting the average of this cut. From the experimental data, $W(x,t)$ was obtained via a Hilbert transformation. The resulting $|C(x)| \equiv |C(x,0)|$ is shown in Fig. 4(c) (theory) and 4(d) (experiment). As seen in the figures, $|C(x)|$ drops very fast to approximately zero, demonstrating that after this distance, the individual oscillators behave uncorrelated. Note that the fluctuations of $|C(x)|$ are due to the finiteness of the sample. We point out that neither in the theoretical nor in the experimental profiles, amplitude defects are present. This situation contrasts with the so-called localized turbulence found under linear global coupling.[43]

III. CONCLUSIONS

In this article, we demonstrate that two-dimensional chimera states and other spatial symmetry breakings may spontaneously occur in systems with nonlinear global coupling, both theoretically and experimentally. Simulations of an ensemble of Stuart-Landau oscillators, coupled solely via the nonlinear global coupling, provide evidence that a nonlocality of the coupling is dispensable for the formation of chimera states. The spontaneity of the formation of chimeras is astonishing and affirms earlier theoretical observations.[25]

The theoretical description is very general and a nonlinear global coupling seems to be essential for the modelling of subharmonic cluster patterns, where the clusters oscillate at a lower frequency than the homogeneous mode.[20] Subharmonic clusters were observed in a number of experiments,[19,44–47] suggesting that also the type of symmetry breaking described here, especially the chimera state, may occur spontaneously in many physical and chemical systems. Furthermore, as shown in Ref. 48, the proposed nonlinearity of the global coupling may also arise effectively in systems of linearly coupled relaxational oscillators.

ACKNOWLEDGMENTS

We thank Andreas Heinrich and Martin Wiegand for assistance on the experiments and Moritz Müller for his work on the simulation program. Financial support from the *Deutsche Forschungsgemeinschaft* (Grant No. KR1189/12-1), the *Institute for Advanced Study, Technische Universität München* funded by the German Excellence Initiative and the cluster of excellence *Nanosystems Initiative Munich (NIM)* is gratefully acknowledged.

APPENDIX: NUMERICAL AND EXPERIMENTAL METHODS

1. Simulations of the ensemble of Stuart-Landau oscillators

We numerically solve Eqs. (1) in the main text using an implicit Adams method with timestep $dt = 0.01$. The system consists of $N = 1000$ oscillators, initialized with random real numbers (with the condition on their average fulfilled). Note that the equation is dimensionless.

2. Simulations of the modified complex Ginzburg-Landau equation

Simulations of Eq. (2) in the main text are carried out using a pseudospectral method and an exponential time stepping algorithm.[49] We use 512×512 Fourier modes and a system size of $L = 800$. Note that the equation is dimensionless. The system is initialized with a two-dimensional

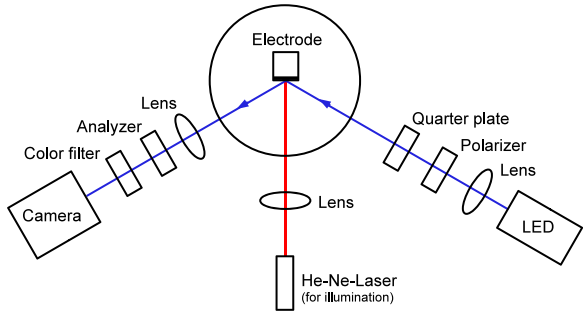

FIG. 5. Optical setup of the custom-made ellipsometric microscope. The blue (dark gray) line represents the light path for the imaging and the red (light gray) line for the illumination.

circular perturbation and additional noise. The dynamics is analyzed between $t = 500$ and $t = 1000$ and we use a computational timestep of $\Delta t = 0.05$.

3. Experiments

The experiments are carried out in a custom made PTFE three electrode electrochemical cell with a monocrystalline n-Si ((111) surface, 3–5 Ωcm) working electrode, a $Hg|Hg_2SO_4$ reference electrode and a ring-shaped platinum counter electrode placed symmetrically in front of the working electrode.[19] The working electrode has an ohmic aluminum back contact annealed at 250 °C for 15 min and is otherwise prepared as described in an earlier work.[50] We use a NH_4F solution as electrolyte, adjust the pH value by adding H_2SO_4, and stir with a magnetic stirrer at about 10 Hz. For illumination, a He-Ne Laser (633 nm) is used, whose intensity I is tuned by a polarizer. For all experiments, a voltage of 8.65 V vs. SHE (Standard Hydrogen Electrode) is applied and the current response is recorded. For the spatially resolved ellipsometric imaging, elliptically polarized light (LED, 470 nm) is reflected from the working-electrode surface at an angle of 70°, close to the Brewster angle, which is to maximize the contrast. The reflected light then passes another polarizer that converts changes of the polarization upon interaction with the surface into intensity changes, and is imaged on a CCD chip (640 × 480 pixels). For a schematic setup, see Fig. 5.

The data are then recorded using a suitable LabVIEW program and analyzed with MATLAB. The parameters varied in the experiments are: the concentration of NH_4F, $[NH_4F]$, the surface area of the working electrode, A, the external resistance, R_{ext}, and the illumination intensity, I. Values read: $[NH_4F] = 35\,\text{mM}$, $\text{pH} = 1$, $A = 22.73\,\text{mm}^2$, $R_{ext} = 40\,\text{k}\Omega$, and $I \simeq 0.7\,\text{mW/cm}^2$ (two-phase clusters), $[NH_4F] = 50\,\text{mM}$, $\text{pH} = 2.3$, $A = 23.06\,\text{mm}^2$, $R_{ext} = 0\,\Omega$, and $I \simeq 1\,\text{mW/cm}^2$ (sub-clustering), and $[NH_4F] = 50\,\text{mM}$, $\text{pH} = 3$, $A = 22.42\,\text{mm}^2$, $R_{ext} = 0\,\Omega$, and $I \simeq 0.5\,\text{mW/cm}^2$ (chimera).

[1]Y. Kuramoto and D. Battogtokh, "Coexistence of coherence and incoherence in nonlocally coupled phase oscillators," Nonlinear Phenom. Complex Syst. **5**, 380–385 (2002).
[2]A. S. Mikhailov and K. Showalter, "Control of waves, patterns and turbulence in chemical systems," Phys. Rep. **425**, 79–194 (2006).
[3]D. M. Abrams and S. H. Strogatz, "Chimera states for coupled oscillators," Phys. Rev. Lett. **93**, 174102 (2004).
[4]S.-i. Shima and Y. Kuramoto, "Rotating spiral waves with phase-randomized core in nonlocally coupled oscillators," Phys. Rev. E **69**, 036213 (2004).
[5]E. A. Martens, C. R. Laing, and S. H. Strogatz, "Solvable model of spiral wave chimeras," Phys. Rev. Lett. **104**, 044101 (2010).
[6]G. C. Sethia, A. Sen, and F. M. Atay, "Clustered chimera states in delay-coupled oscillator systems," Phys. Rev. Lett. **100**, 144102 (2008).
[7]D. M. Abrams, R. Mirollo, S. H. Strogatz, and D. A. Wiley, "Solvable model for chimera states of coupled oscillators," Phys. Rev. Lett. **101**, 084103 (2008).
[8]I. Omelchenko, Y. Maistrenko, P. Hövel, and E. Schöll, "Loss of coherence in dynamical networks: Spatial chaos and chimera states," Phys. Rev. Lett. **106**, 234102 (2011).
[9]I. Omelchenko, B. Riemenschneider, P. Hövel, Y. Maistrenko, and E. Schöll, "Transition from spatial coherence to incoherence in coupled chaotic systems," Phys. Rev. E **85**, 026212 (2012).
[10]S. Nkomo, M. R. Tinsley, and K. Showalter, "Chimera states in populations of nonlocally coupled chemical oscillators," Phys. Rev. Lett. **110**, 244102 (2013).
[11]I. Omelchenko, O. E. Omel'chenko, P. Hövel, and E. Schöll, "When nonlocal coupling between oscillators becomes stronger: Patched synchrony or multichimera states," Phys. Rev. Lett. **110**, 224101 (2013).
[12]N. C. Rattenborg, C. J. Amlaner, and S. L. Lima, "Behavioral, neurophysiological and evolutionary perspectives on unihemispheric sleep," Neurosci. Biobehav. Rev. **24**, 817–842 (2000).
[13]C. G. Mathews, J. A. Lesku, S. L. Lima, and C. J. Amlaner, "Asynchronous eye closure as an anti-predator behavior in the western fence lizard (*Sceloporus occidentalis*)," Ethology **112**, 286–292 (2006).
[14]T. P. Vogels, K. Rajan, and L. F. Abbott, "Neural network dynamics," Annu. Rev. Neurosci. **28**, 357–376 (2005).
[15]D. Barkley and L. S. Tuckerman, "Computational study of turbulent laminar patterns in Couette flow," Phys. Rev. Lett. **94**, 014502 (2005).
[16]M. R. Tinsley, N. Simbarashe, and K. Showalter, "Chimera and phase-cluster states in populations of coupled chemical oscillators," Nat. Phys. **8**, 662–665 (2012).
[17]A. M. Hagerstrom, T. E. Murphy, R. Roy, P. Hövel, I. Omelchenko, and E. Schöll, "Experimental observation of chimeras in coupled-map lattices," Nat. Phys. **8**, 658–661 (2012).
[18]E. A. Martens, S. Thutupalli, A. Fourrire, and O. Hallatschek, "Chimera states in mechanical oscillator networks," Proc. Natl. Acad. Sci. U.S.A. (2013).
[19]I. Miethe, V. García-Morales, and K. Krischer, "Irregular subharmonic cluster patterns in an autonomous photoelectrochemical oscillator," Phys. Rev. Lett. **102**, 194101 (2009).
[20]V. García-Morales, A. Orlov, and K. Krischer, "Subharmonic phase clusters in the complex Ginzburg-Landau equation with nonlinear global coupling," Phys. Rev. E **82**, 065202 (2010).
[21]Y. Kuramoto, *Chemical Oscillations, Waves, and Turbulence* (Dover Publications, Inc., Mineola, New York, 2003).
[22]G. C. Sethia, A. Sen, and G. L. Johnston, "Amplitude-mediated chimera states," Phys. Rev. E **88**, 042917 (2013).
[23]M. Wickramasinghe and I. Z. Kiss, "Spatially organized dynamical states in chemical oscillator networks: Synchronization, dynamical differentiation, and chimera patterns," PLoS One **8**, e80586 (2013).
[24]M. Wolfrum and O. E. Omel'chenko, "Chimera states are chaotic transients," Phys. Rev. E **84**, 015201 (2011).
[25]O. E. Omel'chenko, Y. L. Maistrenko, and P. A. Tass, "Chimera states: The natural link between coherence and incoherence," Phys. Rev. Lett. **100**, 044105 (2008).
[26]N. Nakagawa and Y. Kuramoto, "From collective oscillations to collective chaos in a globally coupled oscillator system," Physica D **75**, 74–80 (1994).
[27]H. Daido and K. Nakanishi, "Diffusion-induced inhomogeneity in globally coupled oscillators: Swing-by mechanism," Phys. Rev. Lett. **96**, 054101 (2006).
[28]K. Kaneko, "Clustering, coding, switching, hierarchical ordering, and control in a network of chaotic elements," Physica D **41**, 137–172 (1990).
[29]I. S. Aranson and L. Kramer, "The world of the complex Ginzburg-Landau equation," Rev. Mod. Phys. **74**, 99–143 (2002).
[30]R. Memming and G. Schwandt, "Anodic dissolution of silicon in hydrofluoric acid solutions," Surf. Sci. **4**, 109–124 (1966).
[31]M. Matsumura and S. R. Morrison, "Anodic properties of n-Si and n-Ge electrodes in HF solution under illumination and in the dark," J. Electroanal. Chem. **147**, 157–166 (1983).

[32]S. Cattarin, I. Frateur, M. Musiani, and B. Tribollet, "Electrodissolution of p-Si in acidic fluoride media: Modeling of the steady state," J. Electrochem. Soc. **147**, 3277–3282 (2000).
[33]X. G. Zhang, *Electrochemistry of Silicon and Its Oxides* (Kluwer Academic, New York, 2001).
[34]D. J. Blackwood, A. Borazio, R. Greef, L. M. Peter, and J. Stuper, "Electrochemical and optical studies of silicon dissolution in ammonium fluoride solutions," Electrochim. Acta **37**, 889–896 (1992).
[35]J.-N. Chazalviel, C. da Fonseca, and F. Ozanam, "*In situ* infrared study of the oscillating anodic dissolution of silicon in fluoride electrolytes," J. Electrochem. Soc. **145**, 964–973 (1998).
[36]F. Yahyaoui, T. Dittrich, M. Aggour, J.-N. Chazalviel, F. Ozanam, and J. Rappich, "Etch rates of anodic silicon oxides in dilute fluoride solutions," J. Electrochem. Soc. **150**, B205–B210 (2003).
[37]J.-N. Chazalviel, "Ionic processes through the interfacial oxide in the anodic dissolution of silicon," Electrochim. Acta **37**, 865–875 (1992).
[38]M. Aggour, M. Giersig, and H. Lewerenz, "Interface condition of n-Si(111) during photocurrent oscillations in NH_4F solutions," J. Electroanal. Chem. **383**, 67–74 (1995).
[39]H. H. Rotermund, G. Haas, R. U. Franz, R. M. Tromp, and G. Ertl, "Imaging pattern formation in surface reactions from ultrahigh vacuum up to atmospheric pressure," Science **270**, 608–610 (1995).
[40]I. Miethe, "Spatio-temporal pattern formation during the anodic electrodissolution of silicon in ammonium fluoride solution," PhD Thesis (TU München, 2010).
[41]K. Krischer, H. Varela, A. Bîrzu, F. Plenge, and A. Bonnefont, "Stability of uniform electrode states in the presence of ohmic drop compensation," Electrochim. Acta **49**, 103–115 (2003).
[42]A. De Wit, D. Lima, G. Dewel, and P. Borckmans, "Spatiotemporal dynamics near a codimension-two point," Phys. Rev. E **54**, 261–271 (1996).
[43]D. Battogtokh, A. Preusser, and A. Mikhailov, "Controlling turbulence in the complex Ginzburg-Landau equation II. Two-dimensional systems," Physica D **106**, 327–362 (1997).
[44]H. Varela, C. Beta, A. Bonnefont, and K. Krischer, "A hierarchy of global coupling induced cluster patterns during the oscillatory H_2-electrooxidation reaction on a Pt ring-electrode," Phys. Chem. Chem. Phys. **7**, 2429–2439 (2005).
[45]V. K. Vanag, A. M. Zhabotinsky, and I. R. Epstein, "Pattern formation in the Belousov–Zhabotinsky reaction with photochemical global feedback," J. Phys. Chem. A **104**, 11566–11577 (2000).
[46]M. Kim, M. Bertram, M. Pollmann, A. von Oertzen, A. S. Mikhailov, H. H. Rotermund, and G. Ertl, "Controlling chemical turbulence by global delayed feedback: Pattern formation in catalytic CO oxidation on Pt(110)," Science **292**, 1357–1360 (2001).
[47]M. Pollmann, M. Bertram, and H. H. Rotermund, "Influence of time delayed global feedback on pattern formation in oscillatory CO oxidation on Pt(110)," Chem. Phys. Lett. **346**, 123–128 (2001).
[48]I. Z. Kiss, Y. Zhai, and J. L. Hudson, "Predicting mutual entrainment of oscillators with experiment-based phase models," Phys. Rev. Lett. **94**, 248301 (2005).
[49]S. M. Cox and P. C. Matthews, "Exponential time differencing for stiff systems," J. Comput. Phys. **176**, 430–455 (2002).
[50]K. Schönleber and K. Krischer, "High-amplitude versus low-amplitude current oscillations during the anodic oxidation of p-type silicon in fluoride containing electrolytes," Chem. Phys. Chem. **13**, 2989–2996 (2012).